

1 **Nickel Supported on Mesoporous Zirconium Oxide by Atomic Layer Deposition: Initial**  
2 **Fixed-Bed Reactor Study**

3 Pauline Voigt<sup>1,2</sup>, Eero Haimi<sup>1</sup>, Jouko Lahtinen<sup>3</sup>, You Wayne Cheah<sup>1,4</sup>, Eveliina Mäkelä<sup>1</sup>, Tiia  
4 Viinikainen<sup>1</sup>, Riikka L. Puurunen<sup>1\*</sup>

5 <sup>1</sup> *Department of Chemical and Metallurgical Engineering, Aalto University School of Chemi-  
6 cal Engineering, Espoo, P.O. Box 16100, FI-00076 AALTO, Finland*

7 <sup>2</sup> *Institute for Inorganic Chemistry I, Technische Universität Dresden, Bergstraße 66, 01069  
8 Dresden, Germany*

9 <sup>3</sup> *Department of Applied Physics, Aalto University School of Science, P.O. Box 15100, FI-  
10 00076 Aalto, Finland*

11 <sup>4</sup> *Faculty of Science and Engineering, Åbo Akademi University, FI-20500 Turku, Finland*

12 \* *corresponding author: [riikka.puurunen@aalto.fi](mailto:riikka.puurunen@aalto.fi), +358 50 337 8161*

13 *ORCID numbers: Jouko Lahtinen 0000-0002-1192-9945, Eveliina Mäkelä 0000-0001-9438-  
14 8111, Riikka L. Puurunen: 0000-0001-8722-4864*

15 **Acknowledgements**

16 This manuscript is partly based on the Berzelius Prize plenary lecture by R.L.P. at the Nordic  
17 Symposium on Catalysis, August 2018, Copenhagen, Denmark. The results are to be reported  
18 in the M.Sc. thesis of P.V. at Technische Universität Dresden, supervised by Prof. Stefan  
19 Kaskel. Daniel Settipani is acknowledged for helping P.V. with the ALD practicalities, and  
20 Ilkka Välimaa for helping Y.W.C. with XRF. Dr. Yingnan Zhao is thanked for valuable in-  
21 sights on the DRIFT spectroscopy experiments. Information on early molecular layering ref-  
22 erences has been collectively gathered in the Virtual Project on the History of ALD. Y.W.C.  
23 thanks Åbo Akademi University for the 2018 partial internship grant. Saint-Gobain Ceramic  
24 Materials GmbH provided the zirconia used in this work free of charge. This research has

25 benefited from the Bioeconomy and RawMatTERS Finland (RAMI) research infrastructures  
26 at Aalto University and used facilities at OtaNano - Nanomicroscopy Center (Aalto-NMC).

27

## 28 **Abstract**

29 Atomic layer deposition (ALD) is gaining attention as a catalyst preparation method able to  
30 produce metal (oxide, sulphide, etc.) nanoparticles of uniform size down to single atoms. This  
31 work reports our initial experiments to support nickel on mesoporous zirconia. Nickel  
32 (2,2,6,6-tetramethyl-3,5-heptanedionato)<sub>2</sub> [Ni(thd)<sub>2</sub>] was reacted in a fixed-bed ALD reactor  
33 with zirconia, characterised with BET surface area of 72 m<sup>2</sup>/g and mean pore size of 14 nm.  
34 According to X-ray fluorescence measurements, the average nickel loading on the top part of  
35 the support bed was on the order of 1 wt-%, corresponding to circa one nickel atom per square  
36 nanometre. Cross-sectional scanning electron microscopy combined with energy-dispersive  
37 spectroscopy confirmed that in the top part of the fixed support bed, nickel was distributed  
38 throughout the zirconia particles. X-ray photoelectron spectroscopy indicated the nickel oxi-  
39 dation state to be two. Organic thd ligands remained complete on the surface after the Ni(thd)<sub>2</sub>  
40 reaction with zirconia, as followed with diffuse reflectance infrared Fourier transform spec-  
41 troscopy. The ligands could be fully removed by oxidation at 400 °C. These initial results  
42 indicate that nickel catalysts on zirconia can likely be made by ALD. Before catalytic testing,  
43 in addition to increasing the nickel loading by repeated ALD cycles, optimization of the pro-  
44 cess parameters is required to ensure uniform distribution of nickel throughout the support  
45 bed and within the zirconia particles.

46

## 47 Introduction

48 Atomic layer deposition (ALD) is a thin film growth method that allows the preparation of  
49 uniform inorganic material layers on arbitrarily complex three-dimensional structures. The  
50 three-dimensional uniformity, also termed “conformality,” is a consequence of the systematic  
51 use of repeated, self-terminating (saturating, irreversible), separated gas–solid reactions of at  
52 least two compatible compounds [1-6]. While the principles of ALD were formulated already  
53 in the 1960s and 1970s, independently twice [7-14], it was in the 1990s that ALD was pro-  
54 moted as a tool for nanotechnology [15] and during the 2000s that ALD has enabled the con-  
55 tinuation of Moore’s law of transistor miniaturisation [16]. By the end of 2010, over 700 two-  
56 reactant ALD processes had been developed [17]. The Finnish inventor of ALD, Dr. Tuomo  
57 Suntola, received the prestigious Millennium Technology Prize in 2018 [18].

58  
59 ALD can coat conformally porous high-surface-area catalyst supports by catalytically active  
60 materials. The first reports of the use of ALD for preparing supported heterogeneous catalysts  
61 are from the Soviet Union in the early 1970s, typically reported under the name “molecular  
62 layering” [12,19-24]. In 1990s, there was a strong industry-driven effort for ALD for catalysis  
63 in Finland; the technique was then called “atomic layer epitaxy” [11,25-32]. Interest in ALD  
64 for the preparation of supported heterogeneous catalysts has again been increasing during the  
65 past decade [33-39]. The current interest in ALD is based for example in the ability of ALD to  
66 prepare (close to) monodisperse metal particles; to make overcoatings to temper the activity  
67 of highly active but non-selective sites; and to prepare single-atom catalysts. The solvent-free  
68 nature of ALD is generally regarded an environmental advantage, and scaling up the catalyst  
69 preparation should be feasible.

70

71 Various reactor designs can be used for coating particles by ALD. Many of the early ALD  
72 catalyst works in the Soviet Union and Finland employed fixed-bed reactors [12,24,31];  
73 fixed-bed reactors have recently re-gained interest [37]. Also fluidised bed [40-42] and rotary  
74 bed [43,44] reactors have been used. Thanks to the advances on ALD in the field of microe-  
75 lectronics, many groups have recently used a reactor set-up where a tray of powder is placed  
76 in a reactor optimised for thin film growth [34]. Whatever the reactor type, the strength of  
77 ALD is best employed when the whole particle bed is coated with a uniform, conformal mate-  
78 rial layer. Attainment of saturation is not self-evident [39,45]; conformality in extreme aspect  
79 ratios needs process tuning and should be verified.

80

81 Nickel is a well known hydrogenation catalyst. Supported nickel catalysts were among the  
82 first ALD catalysts studied in Finland in the 1990s, with focus on toluene hydrogenation  
83 [28,29]. More recently, nickel catalysts have received attention for example in biomass gasifi-  
84 cation, not only because of their low price compared to noble metals, but also because they  
85 are highly active in tar cracking and reforming [46]. Nickel can be used for CO<sub>2</sub> hydrogena-  
86 tion on silica-supported catalysts [47] and aqueous phase reforming of alcohols on zirconia  
87 containing supports [48]. In general, ZrO<sub>2</sub> is considered as an attractive catalyst support due  
88 to its high thermal stability and amphoteric nature [49].

89

90 This work reports an initial study to prepare nickel catalysts on a mesoporous zirconia support  
91 by ALD cycles. We used Ni(thd)<sub>2</sub> (thd = 2,2,6,6-tetramethyl-3,5-heptanedionato), a traditional  
92 ALD reactant [50-53], as the nickel source; and air as the oxygen source. To our best  
93 knowledge, this work is the first to report the ALD modification of mesoporous zirconia with  
94 nickel.

## 95 Experimental

96

### 97 *Materials*

98 The precursor Ni-bis-2,2,6,6-tetramethyl-heptane-3,5-dionate (Ni(thd)<sub>2</sub>) was synthesised from  
99 nickel(II) acetate tetrahydrate (J.T. Baker Chemical, >98%) and 2,2,6,6-Tetramethyl-3,5-  
100 heptanedione (Tokio Chemical Industrie Co., >97%) according to literature methods [53,54]  
101 and purified by sublimation under vacuum before use. Mesoporous zirconium oxide (Saint-  
102 Gobain Norpro, monoclinic <0.2wt% SiO<sub>2</sub>) was crushed and sieved to 250–450 μm particles,  
103 calcined in synthetic air (purity 5.0, Oy AGA Ab) at 600 °C for 10 h and stored in an desicca-  
104 tor.

105

### 106 *N<sub>2</sub> Physisorption*

107 Nitrogen physisorption isotherms were measured at isothermal conditions in liquid nitrogen  
108 (77 K) using a Thermo Fisher Surfer equipment. The fresh, 600 °C heat-treated zirconia sup-  
109 port (0.24 g) was weighted in a quartz tube and evacuated at 350 °C for 3 h (heating ramp  
110 5 °C/min) prior to the measurement. Specific surface area was calculated from the adsorption  
111 isotherm according to the Brunauer-Emmett-Teller (BET) theory using the relative pressure  
112  $p/p_0$  range of 0.2-0.4 [55]. Pore size distribution, mean pore diameter and total pore volume  
113 were calculated using the Barrett-Joyner-Halenda (BJH) method [56].

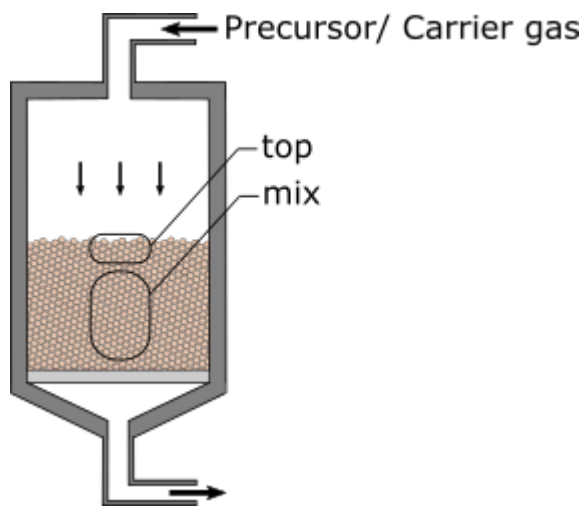
114

### 115 *ALD Procedure*

116 The experiments were carried out using an F-120 flow-type ALD reactor, modified to ac-  
117 commodate a porous high-surface-area materials in a fixed bed (ASM Microchemistry Ltd.,  
118 Finland). The reactor and procedure were similar as described e.g. by Haukka et al. [31].  
119 Schematic illustration of the fixed particle bed is shown in Figure 1. The reaction chamber for

120 powders (diameter 2 cm) was used with the associated filter to hold up to ca. 5 g of support.  
121 The particle bed height was over one centimetre (accurate height not measured). The Ni(thd)<sub>2</sub>  
122 reactant was placed in an open glass boat within the reactor and sublimated at 140 °C, operat-  
123 ed under a moderate vacuum of 0.6-4 mbar (pressure measured after the support bed). Nitro-  
124 gen (>99.99999 %, generated with a Parker HPN2-5000 from air, with less than 10 ppm of  
125 oxygen) was used as a carrier and purging gas, with constant flow rate of 400 sccm. The sup-  
126 port was stabilised at 400 °C for 3 h in a stream of nitrogen. After this, the temperature was  
127 stabilised to the desired reaction temperature (200 °C) and the reactant vapour was led down-  
128 wards through the fixed support bed for 3 h. After the reaction, the sample was purged with  
129 nitrogen at the reaction temperature for 2 h. At the end of the run, the reactor was cooled close  
130 to room temperature before unloading. Samples were taken from the top part of the support  
131 bed and mixing the rest of the material as one sample. The samples were stored in a desicca-  
132 tor.

133



134

135 **Figure 1** A schematic illustration of the fixed-bed F-120 ALD reaction chamber. Samples were separately  
136 taken from the top of the particle bed and mixing the rest of the material as one sample.

137

138 *X-ray Fluorescence*

139 The chemical composition and nickel loading of the prepared materials were measured semi-  
140 quantitatively by X-ray fluorescence (XRF) using a PANalytical AxiosMax Wavelength Dis-  
141 persive X-ray Fluorescence Spectrometer (WD-XRF). The device was equipped with a scin-  
142 tillation detector and a rhodium tube, which operated at 60 kV with a current of 50 mA. The  
143 samples (100-500 mg) in powder form were placed on a supporting thin film using XRF sam-  
144 ple cup (32 mm width).

145

#### 146 *X-ray Photoelectron Spectroscopy*

147 The X-ray photoelectron spectroscopy (XPS) measurements were made using Kratos Axis  
148 Ultra system, equipped with a monochromatic AlK $\alpha$  X-ray source. All measurements were  
149 performed with 0.3 mm x 0.7 mm analysis area and the charge neutraliser on. A wide scan  
150 was performed with 80 eV pass energy and 1 eV energy step. High resolution scans were per-  
151 formed with 20 eV pass energy, 0.1 eV steps size for 5 min for the C 1s, Zr 3d and O 1s and  
152 for 20 min for Ni 2p. The energy calibration was made using the adventitious carbon C1s  
153 component at 284.8 eV. All decompositions were made with CasaXPS using GL(30) peaks  
154 (product of 30% Lorentzian and 70% Gaussian). Information depth in XPS is roughly ten  
155 atomic layers.

156

#### 157 *Scanning Electron Microscopy and Energy-dispersive X-ray Spectrometry*

158 Scanning electron microscopy (SEM) and energy-dispersive X-ray spectrometry (EDS) examina-  
159 tion was carried out using Tescan Mira3 scanning electron microscope fitted with a Thermo Sci-  
160 entific energy-dispersive X-ray spectrometer. The EDS system was equipped with silicon drift  
161 detector (SDD). In sample preparation, mesoporous Ni(thd)<sub>2</sub>-modified zirconia particles were  
162 mounted in epoxy resin utilizing vacuum impregnation. The cured mounts were ground and pol-  
163 ished to expose cross-sections of the particles at the face of specimen. Subsequently, specimens

164 were coated with carbon to prevent charging under the electron beam. In the SEM and EDS exam-  
165 ination, electron accelerating voltage of 15 keV was used. First, qualitative elemental analysis was  
166 performed to identify elements present in the specimen. Secondly, EDS line scans were performed  
167 across a selected Ni(thd)<sub>2</sub>-modified zirconia particle. The length of the line was 600 μm including  
168 100 measurement points. Integration of 40 scans was utilised to improve precision of the meas-  
169 urement. Estimated detection limit of EDS is 0.1-0.3 wt-%.

170

### 171 ***Thermogravimetric Analysis (TGA)***

172 The thermal properties of the nickel-modified zirconia were studied with ambient pressure  
173 thermogravimetric analysis (TGA) with the TGA Q500 (TA Instruments, USA). Heating rate  
174 of 10 °C/min and temperature range of 30-600 °C were used. To reduce the amount of mois-  
175 ture, the sample was pre-heated ex situ for 2 h in air at 200 °C before the TGA analysis, and  
176 then quickly transferred into the TGA equipment. The TGA analysis was started with heating  
177 in nitrogen up to 200 °C and holding for 1h, after which the gas was changed to oxygen and  
178 heating was continued until 600 °C.

179

### 180 ***Diffuse Reflectance Infrared Fourier Transform (DRIFT) spectroscopy***

181 Diffuse reflectance infrared Fourier transform (DRIFT) spectroscopy measurements were  
182 made to observe the vanishing of ligands during oxidation at elevated temperatures. Meas-  
183 urements were made with a Nicolet Nexus FTIR spectrometer using a Spectra-Tech in situ  
184 high temperature/high pressure chamber equipped with deuterated triglycine sulphate (DTGS)  
185 detector. The total gas flow was kept at 50 ml/min throughout the measurement. The sample-  
186 holder-cup was filled with 2/3 pure zirconia (approx. 12 mg) at the bottom and 1/3 Ni(thd)<sub>2</sub>-  
187 modified zirconia (approx. 5 mg) at the top. The applied background was the spectra of an  
188 aluminium mirror (4 cm<sup>-1</sup> resolution, 200 scans) in the in situ cell under nitrogen flow.

189

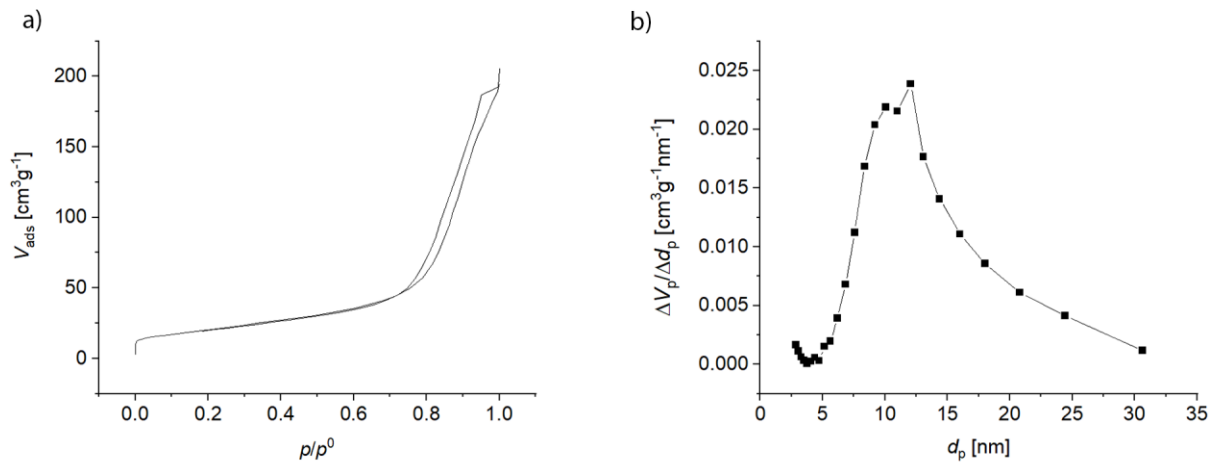
190 First, the sample was pre-heated in the in situ cell in nitrogen (N<sub>2</sub> 99.999 %, AGA) at 200° C  
191 for 3 h, followed by cooling down to 30° C. This was done to reduce moisture, which had  
192 been transferred within the sample to the in situ cell through ambient air. Next, the oxidation  
193 of the surface species was studied by feeding 10% O<sub>2</sub>/N<sub>2</sub> (synthetic air 99.99%) to the cham-  
194 ber at 30 °C followed by increasing the temperature stepwise (steps of 25 °C) to 500 °C. Dur-  
195 ing the stepwise heating of the sample, spectra (4 cm<sup>-1</sup> resolution, wavenumber range 4000-  
196 1000 cm<sup>-1</sup>, 100 scans) were recorded every 25 °C, i.e., approximately every 4 minutes.

## 197 Results and Discussion

### 198 Porosity Characterization of the Support

199 The porosity of the zirconia support heat-treated at 600 °C for 10 h in synthetic air was inves-  
200 tigated through nitrogen physisorption. The N<sub>2</sub> adsorption and desorption isotherms, shown in  
201 Figure 2a, present hysteresis typical for a mesoporous structure [57]. The BET surface area  
202 extracted from the desorption isotherm was 72 m<sup>2</sup>/g and the total pore volume 0.27 cm<sup>3</sup>/g.  
203 The BJH pore size distribution is presented in Figure 2b and shows a mean pore diameter of  
204 13.6 nm.

205



206

207 **Figure 2 Results of nitrogen adsorption and desorption isotherms of the zirconia support: (a) volume of N<sub>2</sub>**  
208 **adsorbed  $V_{\text{ads}}$  (per gram of sample) as function of the relative pressure of nitrogen  $p/p_0$ , and (b) pore size**  
209 **( $d_p$ ) distribution of the zirconia, as analysed with the BJH method.**

210

### 211 **Modification of Zirconia with Ni(thd)<sub>2</sub> by ALD**

212 The Ni(thd)<sub>2</sub> was evaporated at approximately 140 °C and led through a fixed bed of meso-  
213 porous zirconia stabilised at 200 °C. After the modification and cooling down, samples were  
214 taken from the top part of the fixed bed and mixing the rest of the material as one sample (see  
215 Figure 1). According to the semiquantitative XRF measurements, the nickel content in the bed  
216 was on the order of 1 wt-%, with the top sample containing more nickel than the mixed sam-  
217 ple (this had ~60% of top-part content). For ALD, where saturation of the surface with ad-  
218 sorbed species has taken place throughout, a constant nickel concentration would be expected  
219 throughout the support bed. Full saturation had thus not taken place yet.

220

221 After the run, some Ni(thd)<sub>2</sub> was seen in the low-temperature condense tube at the reactor  
222 outlet. As the support bed had not saturated throughout, this means that at the flow conditions

223 used in this work, some Ni(thd)<sub>2</sub> passed the bed unreacted and the reactant usage was there-  
224 fore not optimally efficient.

225

226 To compare with other catalyst ALD studies and also with ALD growth on planar materials, it  
227 is of interest to convert the nickel loading from wt-% to atoms per unit surface area, typically  
228 nm<sup>2</sup> [3]. The nickel surface loading on zirconia with BET surface area of 72 m<sup>2</sup>/g and mean  
229 pore diameter of 14 nm was estimated to be on the order of 1 Ni/nm<sup>2</sup>.

230

231 For further characterization by XPS, SEM-EDS, TGA and DRIFT spectroscopy, a sample  
232 taken from the top part of the support bed was used.

233

#### 234 **XPS**

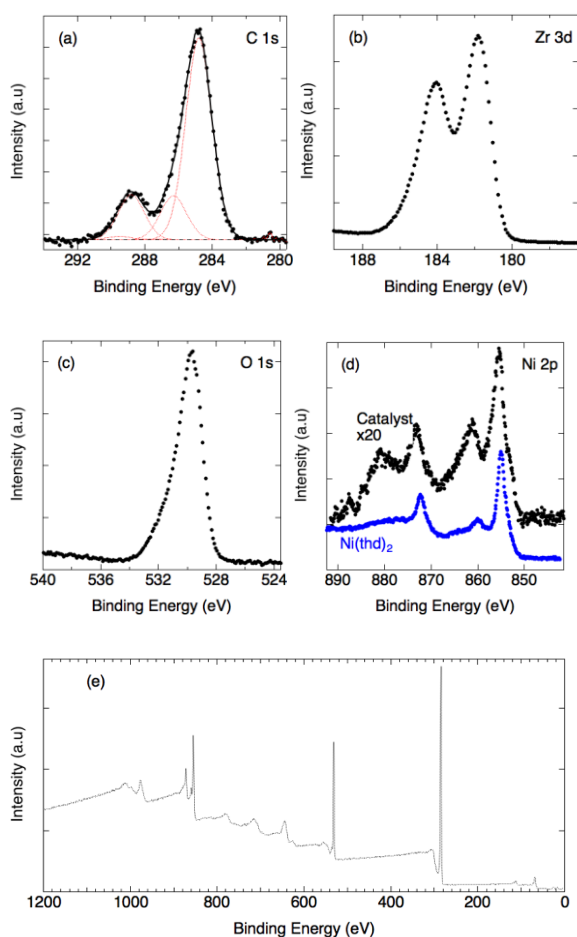
235 The wide spectrum and high resolution spectra of C 1s, Zr 3d, O1s and Ni 2p regions are  
236 shown in Figure 3. Based on the wide scan, the estimated Ni content of the surface layer was  
237 2 at%. For the high resolution spectra we performed a deconvolution of the C 1s spectrum  
238 (Figure 3a) to estimate the binding energy (BE) of the main peak identified as adventitious  
239 carbon in order to get a good BE reference. After fitting, the most intense peak was shifted to  
240 284.8 eV and all the other C-peaks as well as other spectra were corrected with the same  
241 offset. The other components visible in the C 1s spectrum correspond to different C-O -bonds  
242 normally visible after air exposure. The Zr 3p and O 1s spectra shown in Figure 3 are typical  
243 for ZrO<sub>2</sub> with the Zr 3d<sub>5/2</sub> peak close to 182 eV and the O 1s peak close to 530 eV.

244

245 The Ni 2p region shows the 2p<sub>3/2</sub> peak at 855.5 eV and the 2p<sub>1/2</sub> peak at 873.2 eV. Both  
246 peaks have a satellite roughly 6 eV above the main peak. We also measured pure Ni(thd)<sub>2</sub> for  
247 reference, and noticed that the shape of the spectrum is similar, although the intensities of the

248 satellites compared to the main peak are higher in the Ni(thd)<sub>2</sub>-modified zirconia samples.  
249 The satellite intensity in the Ni(thd)<sub>2</sub> increased when the material was left in air for one night  
250 (not shown). We expect this change is due to exposure to humidity. Decomposition of the Ni  
251 spectrum was not performed, but we compared the Ni spectra against reference spectra of NiO  
252 and Ni(OH)<sub>2</sub> [58]. NiO reference shows two components in the 2p<sub>3/2</sub> peak around 855.5 eV  
253 separated by 1.7 eV not visible in our data. The Ni(OH)<sub>2</sub> reference shows one main peak at  
254 855.5 eV and a satellite 6 eV above that, resembling our data. However, the Ni(OH)<sub>2</sub> peaks  
255 reported by [58] are not sufficient to reproduce our data. This indicates slightly different envi-  
256 ronment for Ni atoms than in Ni(OH)<sub>2</sub> or NiO but their oxidation state seems to be two.

257



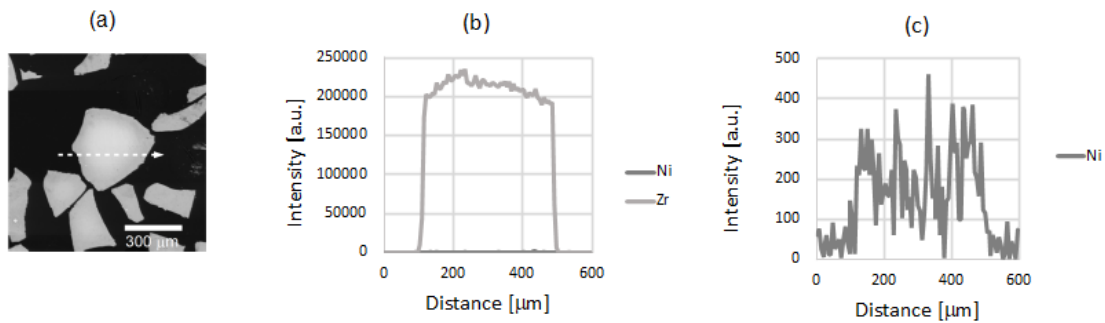
261 **Figure 3 X-ray photoelectron spectra of Ni(thd)<sub>2</sub>-modified zirconia: (a) C 1s, (b) Zr 3d, (c) O1s and (d) Ni**  
262 **2p regions, and (e) the corresponding wide energy spectrum.**

263

## 264 SEM-EDS

265 Initial EDS results showed the presence of Ni in the studied sample. The results concerning Ni  
266 distribution across a zirconia particle are presented in Figure 4. Figure 4a illustrates the position  
267 of EDS line scan on top of backscattered electron image (BSE) of the zirconia particle. Figure 4b  
268 and Figure 4c show measured X-ray intensities as a function of distance along the line scan. The  
269 Figure 4b presents in principle both Zr and Ni intensities for L- and K-lines, respectively. Intensi-  
270 ties coming from Ni are several orders of magnitude lower than intensities coming from Zr, how-  
271 ever, and therefore not distinguishable in the figure. In Figure 4c, the same results for Ni are pre-  
272 sented using smaller intensity axis scaling. The measured X-ray intensities are proportional to the  
273 concentrations of Zr and Ni, respectively. Despite background noise, Ni was detected in zirconia  
274 particles in trace element amount. Furthermore, Ni was observed to be distributed throughout the  
275 zirconia particle.

276



277

278 **Figure 4 (a) Backscattered electron image of zirconia particle showing the position of EDS line scan. (b)**

279 **The EDS line scan of a zirconia particle. (c) The EDS line scan of a zirconia particle with smaller intensity**  
280 **axis scaling.**

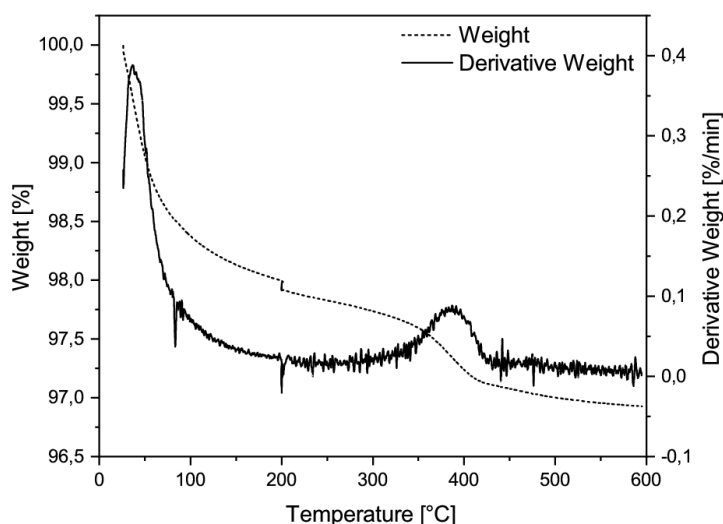
281

## 282 TGA of Nickel-Modified Zirconia

283 After reacting Ni(thd)<sub>2</sub> with zirconia, at least one thd ligand was expected to remain on the  
284 surface. To increase the nickel loading by repeating ALD cycles, the remaining ligands needs  
285 to be removed. This can be done with air at an elevated temperature.

286

287 As a pre-test to find the suitable temperature for removal of the organic thd ligands, TGA  
288 analysis was made for the nickel-modified zirconia; the results are shown in Figure 5. Signifi-  
289 cant weight loss likely due to dehydration and/or dehydroxylation was observed especially up  
290 to 200 °C, and to a small extent after that. An additional weight loss occurred at about 300-  
291 400 °C, which can likely be attributed to removal of the organic thd ligands by oxidation.  
292 Some weight loss continued after 400 °C.



293

294 **Figure 5** TGA curve of Ni(thd)<sub>2</sub>-modified ZrO<sub>2</sub>, heated in N<sub>2</sub> at 200 °C for 1 h to reduce moisture, contin-  
295 ued by heating in O<sub>2</sub> (200-600 °C) with a heating rate of 10 °C/h.

296

### 297 **DRIFT Spectroscopy Observation of Thd Ligand Removal in Air**

298 DRIFT spectroscopy was used to study how the thd ligands were attached to the zirconia  
299 support and for the removal of the thd ligands by oxygen during heating in air.

300

301 The zirconia support was measured as a reference and the spectrum at 30 °C was recorded  
302 after heating in N<sub>2</sub> at 200 °C for 2 hours (spectrum A in Figure 6). The spectrum showed  
303 peaks at 3776 cm<sup>-1</sup> and 3671 cm<sup>-1</sup>, and a small shoulder between these two bands at 3734 cm<sup>-1</sup>.  
304 The peaks at 3776 cm<sup>-1</sup> and 3671 cm<sup>-1</sup> can be assigned to terminal and tribridged OH  
305 groups [59]. The small shoulder at 3734 cm<sup>-1</sup> is likely indicating the existence of bibridged  
306 OH groups [59]. Small bands observed between 1600 and 1000 cm<sup>-1</sup> can be assigned to  
307 residual carbonate groups trapped inside the zirconia bulk [60]. The spectrum of the zirconia  
308 support (spectrum A in Figure 6) also showed moisture on the sample that was expected due  
309 to the pretreatment at low temperature (200 °C). The OH groups have been reported to have  
310 more intense peaks when calcined at 600 °C for 2 hours in air flow [59].

311  
312 The spectrum of Ni(thd)<sub>2</sub>-modified zirconia (pretreated in N<sub>2</sub> at 200 °C for 2 hours and cooled  
313 down to 30 °C) showed several intense peaks (spectrum B in Figure 6), indicating differences  
314 compared to the unmodified support (spectrum A in Figure 6). The presence of adsorbed  
315 ligands on the nickel-modified zirconia is evidenced through the methyl group signals (C-H  
316 stretching and bending vibrations) at 2965-2873 cm<sup>-1</sup> and 1429-1230 cm<sup>-1</sup> [31, 61], as well  
317 as through bands related to the thd ligand at 1600-1488 cm<sup>-1</sup> (C=C and C=O stretching  
318 vibrations) [31]. Compared to the spectrum of the zirconia support (spectrum B in Figure 6),  
319 it can be seen that the terminal and bibridged OH groups (at 3776 and 3734 cm<sup>-1</sup>) have  
320 disappeared and the band for tribridged OH groups (at 3671 cm<sup>-1</sup>) has decreased in the  
321 Ni(thd)<sub>2</sub> reaction. The absence of terminal hydroxyl groups suggests that Ni(thd)<sub>2</sub> consumed  
322 them during the reaction with zirconia; the same likely took place with the bibridging OH  
323 groups. Similarly, in earlier works, it has been reported that OH groups of zirconia, especially  
324 the terminal OH groups, react with the precursor in the ALD reaction of Cr(acac)<sub>3</sub> (acac =  
325 acetylacetonate) and zirconia support [62].

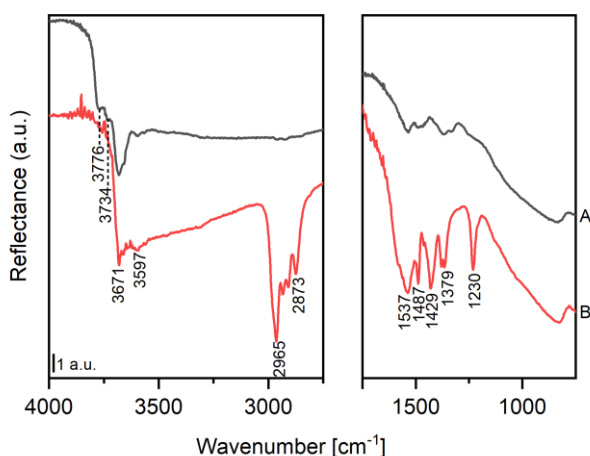
326

327 The DRIFT spectra measured during heating between 30 and 500 °C for the nickel-modified  
328 zirconia are shown in Figure 7. The peaks assigned to the thd ligands stayed largely intact  
329 during heating in air up to 300 °C. At 350 °C, the C-H bands (at 2873-2965 and 1230-1429  
330  $\text{cm}^{-1}$ ) and C-O bands (at 1488-1600  $\text{cm}^{-1}$ ) started to decrease in intensity and at 400 °C these  
331 bands disappeared. Thus, it can be concluded that thd ligands were completely decomposed  
332 via oxidation below 400 °C. These results are in line with those observed earlier for  $\text{Ir}(\text{acac})_3$   
333 and  $\text{Pt}(\text{acac})_2$  on alumina support, where acac ligands were oxidised below 500 °C [63].

334

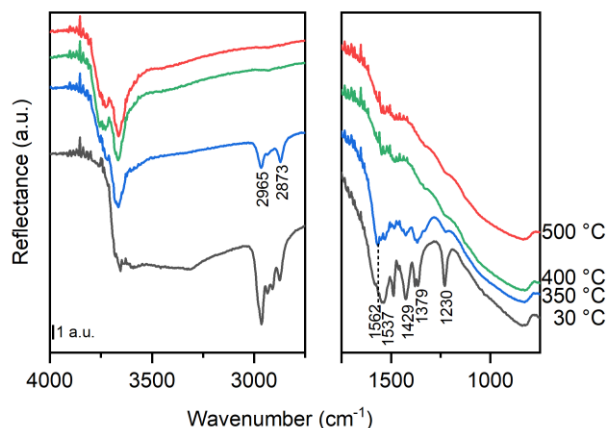
335 To summarize, DRIFT spectroscopy results showed that the reaction of  $\text{Ni}(\text{thd})_2$  with the  
336 zirconia support brought out the expected thd ligands while consuming OH groups. These  
337 ligands can be decomposed and removed in the presence of oxygen by 400 °C, thus  
338 completing the first ALD cycle. The effective removal of ligands by heating in oxygen is  
339 essential for the future use of nickel-modified zirconia as a catalyst since unremoved ligands  
340 would affect the activity of a catalyst.

341



342

343 **Figure 6 DRIFT spectra of (A)  $\text{ZrO}_2$  and (B)  $\text{Ni}(\text{thd})_2$ -modified zirconia at 30 °C after pre-heating at**  
344 **200 °C for 2 h in  $\text{N}_2$ . Spectra shifted vertically for clarity.**



345  
 346 **Figure 7 DRIFT spectra of Ni(thd)<sub>2</sub>-modified zirconia, heated 30-500 °C in 10% O<sub>2</sub>/N<sub>2</sub>. Spectra have been**  
 347 **collected with the sample at the indicated temperature (30-500°C), after initially pre-heating at 200 °C for**  
 348 **2 h and cooling again to 30 °C in N<sub>2</sub> (see Figure 6). Spectra shifted vertically for clarity.**

## 349 Conclusion

350 This article reports our first efforts to support nickel on mesoporous high-surface-area zirco-  
 351 nia by ALD for catalytic purposes. A nickel loading of approximately 1 wt-% was obtained  
 352 by the Ni(thd)<sub>2</sub> reaction at 200 °C using a commercial fixed-bed powder ALD reactor. The  
 353 corresponding surface loading on zirconia (with BET surface area of 72 m<sup>2</sup>/g and mean pore  
 354 diameter of 14 nm) was on the order of 1 Ni/nm<sup>2</sup>. According to XPS, all nickel had oxidation  
 355 state two. According to SEM-EDS cross-sectional observation, at the top part of the fixed  
 356 particle bed, nickel was observed throughout the zirconia particle. Organic thd ligands re-  
 357 mained complete on the surface after the Ni(thd)<sub>2</sub> reaction with zirconia, as followed with  
 358 DRIFT spectroscopy. The first ALD cycle was completed by oxidation, which removed the  
 359 remaining organic ligands at approximately 400 °C and re-created OH groups on the surface.

360  
 361 To use the Ni/zirconia materials as catalysts, it is advisable to ensure full saturation through-  
 362 out the support bed and within the zirconia particles. Full saturation throughout the support

363 bed was not yet attained in this initial work. Further optimization work is needed to ensure  
364 saturation and increase the nickel loading before catalytic testing.

365

## 366 References

367 [1] Suntola T (1989) Atomic Layer Epitaxy. *Mater Sci Reports* 4:261–312 DOI:

368 10.1016/S0920-2307(89)80006-4

369 [2] Leskelä M, Ritala M (2002) Atomic layer deposition (ALD): from precursors to thin film  
370 structures. *Thin Solid Films* 409:138-146 DOI: 10.1016/S0040-6090(02)00117-7

371 [3] Puurunen RL (2005) Surface chemistry of atomic layer deposition: a case study for the  
372 trimethylaluminum/water process. *J Appl Phys* 97:121301 (52 p) DOI: 10.1063/1.1940727

373 [4] George SM (2010) Atomic layer deposition: an overview. *Chem Rev* 110: 111-131 DOI:  
374 10.1021/cr900056b

375 [5] Gao F, Arpiainen S, Puurunen RL (2015) Microscopic silicon-based lateral high-aspect-  
376 ratio structures for thin film conformality analysis, *J Vac Sci Technol A* 33: 101601 (5 p).  
377 DOI: 10.1116/1.4903941

378 [6] Ylilammi M, Ylivaara OME, Puurunen RL (2018) Modeling growth kinetics of thin films  
379 made by atomic layer deposition in lateral high-aspect-ratio structures. *J Appl Phys*  
380 123:205301 (8 p) DOI: 10.1063/1.5028178

381 [7] Aleskovskii VB, Koltsov SI (1965) Some characteristics of molecular layering reactions.  
382 In *Abstract of Scientific and Technical Conference of the Leningrad Technological Institute*  
383 *by Lensovet* (Goskhimizdat, Leningrad, 1965), pp. 67–67 (in Russian).

384 [8] Aleskovskii VB (1974) Chemistry and technology of solids. *J Appl Chem USSR* 47:2207-  
385 2217 [*Zh Prikl Khim* 47:2145-2157]

386 [9] Suntola T, Antson J (1974). Patent FIN 52359 (29 November 1974); corresponds to U.S.  
387 patent 4 058 430 (25 November 1975).

388 [10] Suntola T, Hyvärinen J (1985) Atomic layer epitaxy. *Annu Rev Mater Sci* 15:177-195.

389 [11] Puurunen RL (2014) A short history of Atomic Layer Deposition: Tuomo Suntola's  
390 Atomic Layer Epitaxy. *Chem Vap Deposition* 20:332-344 DOI: 10.1002/cvde.201402012

391 [12] Malygin AA, Drozd VE, Malkov AA, Smirnov VM (2015) From V. B. Aleskovskii's  
392 "Framework" Hypothesis to the Method of Molecular Layering/Atomic Layer Deposition.  
393 *Chem Vap Deposition* 21:216-240 DOI: 10.1002/cvde.201502013

394 [13] Ahvenniemi E, Akbashev AR, Ali S, Bechelany M, Berdova M, Boyadjiev S, Cameron  
395 DC, Chen R, Chubarov M, Cremers V, Devi A, Drozd V, Elnikova L, Gottardi G, Grigoras K,  
396 Hausmann DM, Hwang CS, Jen SH, Kallio T, Kanervo J, Khmel'nitskiy I, Kim DH, Klibanov  
397 L, Koshtyal Y, Krause AOI, Kuhs J, Kärkkänen I, Kääriäinen ML, Kääriäinen T, Lamagna L,  
398 Łapicki AA, Leskelä M, Lipsanen H, Lyytinen J, Malkov A, Malygin A, Mennad A, Militzer  
399 C, Molarius J, Norek M, Özgüt-Akgün Ç, Panov M, Pedersen H, Piallat F, Popov G, Puurunen  
400 RL, Rampelberg G, Ras RHA, Rauwel E, Roozeboom F, Sajavaara T, Salami H, Savin H,  
401 Schneider N, Seidel TE, Sundqvist J, Suyatin DB, Törndahl T, Van Ommen JR, Wiemer C,  
402 Ylivaara OME Yurkevich, O (2017) Review Article: Recommended reading list of early pub-  
403 lications on atomic layer deposition—Outcome of the “Virtual Project on the History of ALD.  
404 *J Vac Sci Technol A* 25:010801 (13 p). DOI: 10.1116/1.4971389.

405 [14] Puurunen RL (2018) Learnings from an Open Science effort: Virtual Project on the His-  
406 tory of ALD. *ECS Trans* 86(6):3-17 DOI: 10.1149/08606.0003ecst

407 [15] Ritala M, Leskelä M (1999) Atomic layer epitaxy—a valuable tool  
408 for nanotechnology? *Nanotechnology* 10:19-24 DOI: 10.1088/0957-4484/10/1/005

409 [16] Bohr MT, Chau RS, Ghani T, Mistry K (2007) The high-k solution. *IEEE Spectrum* 44:  
410 29–35 DOI: 10.1109/MSPEC.2007.4337663

411 [17] Miikkulainen V, Leskelä M, Ritala M, Puurunen RL (2013) Crystallinity of inorganic  
412 films grown by atomic layer deposition: Overview and general trends. *J Appl Phys*  
413 113:021301 (101 p) DOI: 10.1063/1.4757907

414 [18] Technology Academy Finland, May 22, 2018, “2018 Millennium Technology Prize for  
415 Tuomo Suntola – Finnish physicist's innovation enables manufacture and development of  
416 information technology products.” Link: [https://taf.fi/2018/05/22/2018-millennium-  
417 technology-prize-for-tuomo-suntola-finnish-physicists-innovation-enables-manufacture-and-  
418 development-of-information-technology-products/](https://taf.fi/2018/05/22/2018-millennium-technology-prize-for-tuomo-suntola-finnish-physicists-innovation-enables-manufacture-and-development-of-information-technology-products/). Accessed June 29, 2018.

419 [19] Koltsov SI, Smirnov VM, Aleskovskii VB (1970) Influence of the carrier on catalysts  
420 properties. *Kinet Catal* 11:835-841 [Kinet Katal 11:1013-1021, original article in Russian]

421 [20] Volkova AN, Malygin AA, Koltsov SI, Aleskovskii VB (1972) The method of synthesis  
422 of Cr(III) and P(V) oxide layers on the silicagel surface. USSR author's certificate patent  
423 422446 (submitted 31 March 1972) (in Russian).

424 [21] Malygin AA, Volkova AN, Koltsov SI, Aleskovskii VB (1972) The method of synthesis  
425 of vanadium oxide catalyst for the oxidation of organic compounds. USSR author's certificate  
426 patent 422447 (submitted 31 March 1972) (in Russian).

427 [22] Koltsov SI, Smirnov VM, Aleskovskii VB (1973) Influence of carrier on the properties  
428 of catalyst. II. *Kinet Katal* 14:1300-1303 (in Russian)

429 [23] Damyanov D, Mehandjiev D, Obretenov Ts (1975) Preparation of Chromium oxides on  
430 the surface of silica gel by the method of molecular deposition. IV. Catalytic properties. *Proc.*  
431 *III Inter. Symp. Heterogeneous Catalysis-Varna, 1975*, p. 191-195.

432 [24] Malygin AA, Malkov AA, Dubrovenskii SD (1996) Chapter 1.8 The chemical basis of  
433 surface modification technology of silica and alumina by molecular layering method. *Stud*  
434 *Surf Sci Catal* 99:213-236 DOI: 10.1016/S0167-2991(06)81022-0

435 [25] Suntola T, Lakomaa EL, Knuuttila H, Knuuttila P, Krause O, Lindfors S (1990) Process  
436 and apparatus for preparing heterogeneous catalysts. Jan 16, 1990. Patent F184562.

437 [26] Suntola T, Haukka S, Kytökivi A, Lakomaa EL, Lindblad M, Hietala J, Hokkanen H,  
438 Knuuttila H, Knuuttila P, Krause O, Lindfors LP (1991) Method for preparing heterogeneous  
439 catalysts of desired metal content. Jul 16, 1991, Patent F187892.

440 [27] Lakomaa EL (1994) Atomic layer epitaxy (ALE) on porous substrates. *Appl Surf Sci*  
441 75:185-196 DOI: 10.1016/0169-4332(94)90158-9

442 [28] Lindblad M, Lindfors LP, Suntola T (1994) Preparation of Ni/Al<sub>2</sub>O<sub>3</sub> catalysts from vapor  
443 phase by atomic layer epitaxy. *Catal Lett* 27:323–336 DOI: 10.1007/BF00813919

444 [29] Jacobs JP, Lindfors LP, Reintjes JGH, Jylhä O, Brongersma HH (1994) The growth  
445 mechanism of nickel in the preparation of Ni/Al<sub>2</sub>O<sub>3</sub> catalysts studied by LEIS, XPS and cata-  
446 lytic activity. *Catal Lett* 25:315–324 DOI: 10.1007/BF00816311

447 [30] Kytökivi A, Jacobs JP, Hakuli A, Meriläinen J, Brongersma HH (1996) Surface charac-  
448 teristics and activity of chromia/alumina catalysts prepared by atomic layer epitaxy. *J Catal*  
449 162:190-197 DOI: 10.1006/jcat.1996.0276

450 [31] Haukka S, Lakomaa EL, Suntola T (1999) Adsorption controlled preparation of hetero-  
451 geneous catalysts. *Stud Surf Sci Catal* 120:715-750

452 [32] Lakomaa EL, Lindblad M, Kytökivi A, Siro-Minkkinen H, Haukka S, Catalyst pro-  
453 cessing development by atomic layer epitaxy (ALE). In book: *Catalysis in Finland – and ex-  
454 citing pathway*, Suomen katalyysiseura, Otavan Kirjapaino Oy, Keuruu 2013, pp. 93-103.

455 [33] Sun S, Zhang G, Gauquelin N, Chen N, Zhou J, Yang S, Chen W, Meng X, Geng D,  
456 Banis MN, Li R, Ye S, Knights S, Botton GA, Sham TK, Sun X (2013) Single-atom catalysis  
457 using Pt/graphene achieved through atomic layer deposition, *Scientific Reports* 3:1775 (9 p)  
458 DOI: 10.1038/srep01775

459 [34] O'Neill BJ, Jackson DHK, Lee J, Canlas C, Stair PC, Marshall CL, Elam JW, Kuech TF,  
460 Dumesic JA, Huber GW (2015) Catalyst design with atomic layer deposition. ACS Catal  
461 5:1804-1825 DOI: 10.1021/cs501862h

462 [35] Van Bui H, Grillo F, van Ommen JR (2017) Atomic and molecular layer deposition: off  
463 the beaten track. Chem Comm 53:45-71 DOI: 10.1039/c6cc05568k

464 [36] Singh JA, Yang NY, Bent SF (2017) Nanoengineering heterogeneous catalysts by atomic layer  
465 deposition. Annual Review of Chemical and Biomolecular Engineering, Vol. 8, Pages: 41-62 DOI:  
466 10.1146/annurev-chembioeng-060816-101547.

467 [37] Stempel VE, Naumann d'Alnoncourt R, Driess M, Rosowski F (2017) Atomic layer deposition  
468 on porous powders with in situ gravimetric monitoring in a fixed bed reactor setup. Rev Sci Inst  
469 88:074102 (9 p) DOI: 10.1063/1.4992023

470 [38] Cao K, Cai J, Liu X, Chen R (2018), Review article: catalysts design and synthesis via selective  
471 atomic layer deposition, J Vac Sci Technol A 36:010801 (12 p) DOI: 10.1116/1.5000587

472 [39] Onn TM, Küngas R, Fornasiero P, Huang K, Gorte RJ (2018) Atomic layer deposition on  
473 porous materials: problems with conventional approaches to catalyst and fuel cell electrode  
474 preparation. Inorganics 6:34 (20 p) DOI: 10.3390/inorganics6010034

475 [40] Yakovlev SV, Malygin AA, Koltsov SI, Aleskovskii VB, Chesnokov Yu G, Pro-  
476 todyakonov IO (1979) Mathematical model of molecular layering with the aid of a fluidized  
477 bed. J Appl Chem USSR 52:959-963 [Zh Prikl Khim 52:1007-1011]

478 [41] Suvanto M, Rätty J, Pakkanen TA (1999) Carbonyl-precursor-based W/Al<sub>2</sub>O<sub>3</sub> and  
479 CoW/Al<sub>2</sub>O<sub>3</sub> catalysts: characterization by temperature-programmed methods. Catal Lett  
480 62:21-27. DOI: 10.1023/A:1019030518532

481 [42] Suvanto S, Pakkanen TA, Backman L (1999) Controlled deposition of Co<sub>2</sub>(CO)<sub>8</sub> on sili-  
482 ca in a fluidized bed reactor: IR, chemisorption and decomposition studies. Appl Catal A 177:  
483 25-36 DOI: 10.1016/S0926-860X(98)00253-1

484 [43] Cavanagh AS, Wilson CA, Weimer AW, George SM (1999) Atomic layer deposition on  
485 gram quantities of multi-walled carbon nanotubes. *Nanotechnology* 20:255602 (10 p) DOI:  
486 10.1088/0957-4484/20/25/255602

487 [44] Longrie D, Dedytche D, Detavernier C (2013) Reactor concepts for atomic layer deposi-  
488 tion on agitated particles: A review. *J Vac Sci Technol A* 32:010802 (13 p) DOI:  
489 10.1116/1.4851676

490 [45] Munnik P, de Jongh PE, de Jong KP (2015) Recent developments in the synthesis of  
491 supported catalysts. *Chem Rev* 115:6687-6718 DOI: 10.1021/cr500486u

492 [46] Chan FL, Tanksale A (2014) Review of recent developments in Ni-based catalysts for  
493 biomass gasification. *Renew Sustain Energy Rev* 38:428-438 DOI:  
494 10.1016/j.rser.2014.06.011

495 [47] Vogt C, Groeneveld E, Kamsma G, Nachtegaal M, Lu L, Kiely CJ, Berben PH, Meirer F,  
496 Weckhuysen BM, Unravelling structure sensitivity in CO<sub>2</sub> hydrogenation over nickel. *Nat*  
497 *Catal* 1 (2018) 127-134 DOI: 10.1038/s41929-017-0016-y

498 [48] Coronado I, Pitínová M, Karinen R, Reinikainen M, Puurunen RL, Lehtonen J (2018)  
499 Aqueous-phase reforming of Fischer-Tropsch alcohols over nickel-based catalysts to produce  
500 hydrogen: Product distribution and reaction pathways. *Appl. Catal. A* 567:112-121 doi:  
501 10.1016/j.apcata.2018.09.013

502 [49] Jung KT, Bell AT (2000) The effects of synthesis and pretreatment conditions on the  
503 bulk structure and surface properties of zirconia. *J Mol Catal A* 163:27-42 DOI:  
504 10.1016/S1381-1169(00)00397-6

505 [50] Suntola T (1996) Surface chemistry of materials deposition at atomic layer level. *Appl*  
506 *Surf Sci* 100/101:391-398 DOI: 10.1016/0169-4332(96)00306-6

507 [51] Seim H, Mölsä H, Nieminen M, Fjellvåg H, Niinistö L (1997) Deposition of LaNiO<sub>3</sub>  
508 thin films in an atomic layer epitaxy reactor. *J Mater Chem* 7:449-454 DOI:  
509 10.1039/A606316K

510 [52] Lindahl E, Ottosson M, Carlsson J-O (2009) Atomic Layer Deposition of NiO by the  
511 Ni(thd)<sub>2</sub>/H<sub>2</sub>O Precursor Combination. *Chem Vap Deposition* 15:186-191 DOI:  
512 10.1002/cvde.200906762

513 [53] Hagen DJ, Tripathi TS, Karppinen M (2017) Atomic layer deposition of nickel–cobalt  
514 spinel thin films, *Dalton Trans* 46:4796-4805 doi.org/10.1039/C7DT00512A

515 [54] Hammond GS, Nonhebel DC, Wu CHS (1963) Chelates of β-Diketones. V. Preparation  
516 and Properties of Chelates Containing Sterically Hindered Ligands. *Inorg Chem* 2:73-76 DOI:  
517 10.1021/ic50005a021

518 [55] Brunauer S, Emmett PH, Teller E (1938) Adsorption of Gases in Multimolecular Layers.  
519 *J. Am. Chem. Soc.* 60:309–319 DOI: 10.1021/ja01269a023.

520 [56] Barrett EP, Joyner LG, Halenda PP (1951) The Determination of Pore Volume and Area  
521 Distributions in Porous Substances. I. Computations from Nitrogen Isotherms. *J. Am. Chem.*  
522 *Soc.* 73 :373–380 DOI: 10.1021/ja01145a126.

523 [57] Lowell S, Shields JE, Thomas MA, Thommes M (2004) Characterization of Porous Sol-  
524 ids and Powders: Surface Area, Pore Size and Density, (ed) Brian Scarlett, Springer Sci-  
525 ence+Business Media, New York, 351 p. doi: 10.1007/978-1-4020-2303-3

526 [58] Biesinger MC, Payne BP, Lau LWM, Gerson A, Smart RSC (2009) X-ray photoelectron  
527 spectroscopic chemical state quantification of mixed nickel metal, oxide and hydroxide sys-  
528 tems. *Surf Interface Anal* 41:324-332 DOI: 10.1002/sia.3026

529 [59] Viinikainen T, Rönkkönen H, Bradshaw H, Stephenson H, Airaksinen S, Reinikainen M,  
530 Simell P, Krause O (2009) Acidic and basic surface sites of zirconia-based biomass  
531 gasification as clean-up catalysts. *Appl Catal A* 362:169-177 10.1016/j.apcata.2009.04.037

- 532 [60] Guglielminotti E (1990) Infrared study of syngas adsorption on zirconia. *Langmuir*  
533 6:1455-1460 DOI: 10.1021/la00099a005
- 534 [61] Nakamoto K, McCarthy PJ, Martell AE (1961) Infrared Spectra of Metal Chelate Com-  
535 pounds. III. Infrared Spectra of Acetylacetonates of Divalent Metals. *J Am Chem Soc*  
536 83:1272-1276
- 537 [62] Korhonen ST, Bañares MA, Fierro JLG, Krause AOI (2007) Adsorption of methanol as a  
538 probe for surface characteristics of zirconia-, alumina-, and zirconia/alumina-supported chro-  
539 mia catalysts. *Catal Today* 126:235–247. DOI: 10.1016/j.cattod.2007.01.008
- 540 [63] Vuori H, Lindblad M, Krause AOI (2006) Preparation of noble metal catalysts by atomic  
541 layer deposition: FTIR studies. *Stud Surf Sci Catal* 162:505-512 DOI: 10.1016/S0167-  
542 2991(06)80946-8